

Macrocyclic γ -Cyclodextrin Confined Polymeric Chromophore Ultralong Phosphorescence Energy Transfer

Xin-Kun Ma, Qingwen Cheng, Xiaolu Zhou, and Yu Liu*



Cite This: *JACS Au* 2023, 3, 2036–2043



Read Online

ACCESS |



Metrics & More



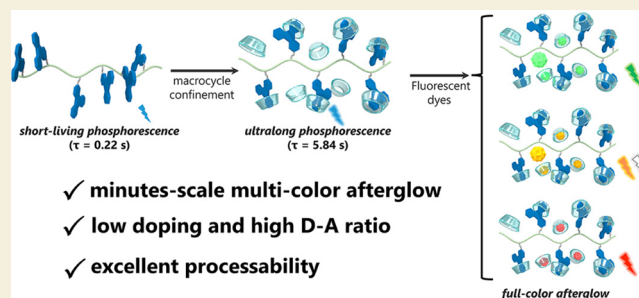
Article Recommendations



Supporting Information

ABSTRACT: A multicolor persistent luminescence solid polymeric system based on macrocycle-confined phosphorescence energy transfer was constructed with γ -cyclodextrin (γ -CD) and poly(vinyl alcohol) modified by triphenylene derivative (TP-PVA). Attributed to the fact that macrocycles effectively suppress the aggregation of guests and form a rigid environment via coassembling with the polymer, the phosphorescence lifetime of the yielded polymeric films is prolonged from 0.22 to 5.84 s, accompanied by a visible afterglow of more than 1 min. Furthermore, upon doping with several commercial dyes, full-color afterglow emissions with a duration of more than 50 s are realized through phosphorescence energy transfer. Notably, the multicolor-emitting-afterglow materials are successfully exploited for noctilucent lighting and anticounterfeiting ink.

KEYWORDS: cyclodextrin, phosphorescence, energy transfer, full-color luminescence, anticounterfeiting



INTRODUCTION

Ultralong lifetime luminescent materials have received tremendous attention due to their potential applications such as flexible electronics, anticounterfeiting, information storage, etc.^{1–5} Organic phosphorescence materials have unique features such as excellent optical properties and good processability.^{6–8} Many brilliant strategies have been developed to improve organic phosphorescence performance, such as polymerization,^{9–14} crystallization,^{15–17} and supramolecular assembly.^{18–23} Prominently, the macrocycle-confined supramolecular assembly has emerged as an alternative and preferable choice for constructing efficient phosphorescent materials.^{24,25} However, most phosphorescence systems based on host–guest complexes are driven by electrostatic interactions; for example, cucurbiturils prefer positively charged guests more than uncharged guests. On the contrary, macrocyclic molecule cyclodextrins consisting of glucose units have a stable hydrophobic cavity, which prefers to accommodate uncharged or negatively charged guests, and the abundant hydroxyl provides the ideal environment to suppress the nonradiative transition for phosphors.^{26–29} Although good results have been realized via various enhancement strategies, the afterglow duration of most organic phosphorescence materials is still on the seconds-scale. In contrast, systems with minute-scale afterglow emission are still in demand and rare.

Developing variable full-color organic persistent luminescence materials is of considerable practical importance. Doping polymeric matrices with various chromophores or suitable triplet energy donors and acceptors (D-A) has been proven to be

a concise approach to obtaining multicolor luminescent materials.^{30–37} However, because long-lived triplet excitons are sensitive to aggregation, molecular motion, and other quenchers, in phosphor-doped systems or D-A-doped phosphorescence energy transfer systems, the performance of long-lived luminescence would suffer severe losses when the chromophores are at a high doping ratio. Thus, we envision that introducing cyclodextrins into the polymeric phosphorescence system could be an effective strategy to inhibit the quenching of chromophores at high concentrations and improve the performance of afterglow emission.

To validate our hypothesis, we designed and constructed solid supramolecular polymers based on cyclodextrin's multiple-confined assembly. Concretely, through the synergistic assembly of poly(vinyl alcohol) (PVA) and γ -cyclodextrin (γ -CD), the triphenylene (TP)-PVA/ γ -CD films display ultralong blue phosphorescence emission (lifetime up to 5.84 s), which is the record result among the reported afterglow polymers (Scheme 1).³⁴ Remarkably, in the presence of γ -CD, the ultralong phosphorescence exhibits excellent stability at high phosphor doping ratios; specifically, the quenching concentration of the phosphorescence lifetime is increased by more than 15-fold

Received: May 23, 2023

Revised: June 27, 2023

Accepted: June 27, 2023

Published: July 11, 2023



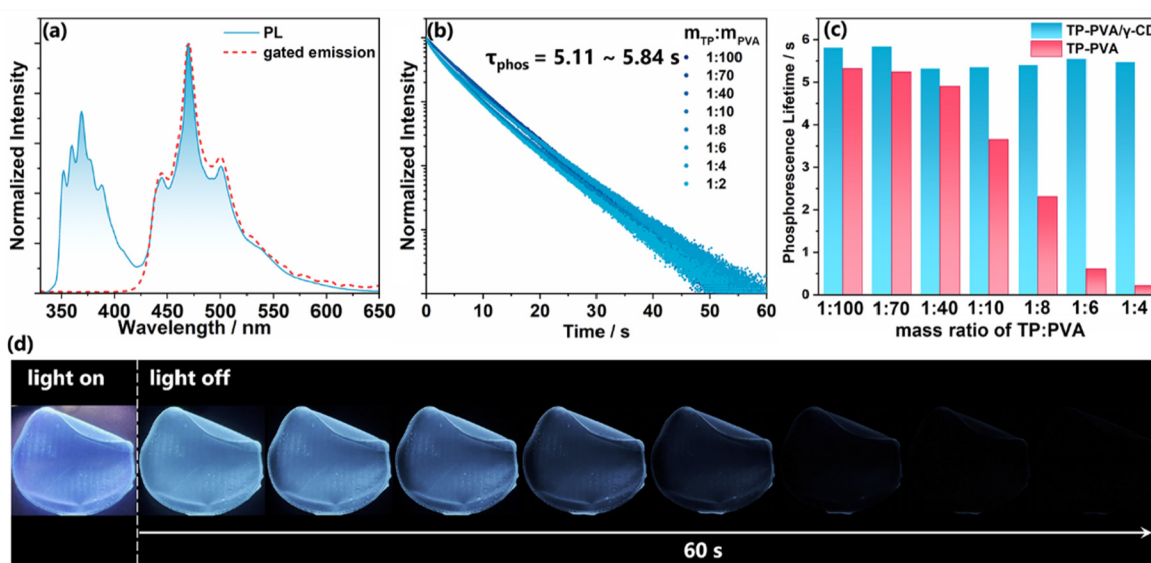
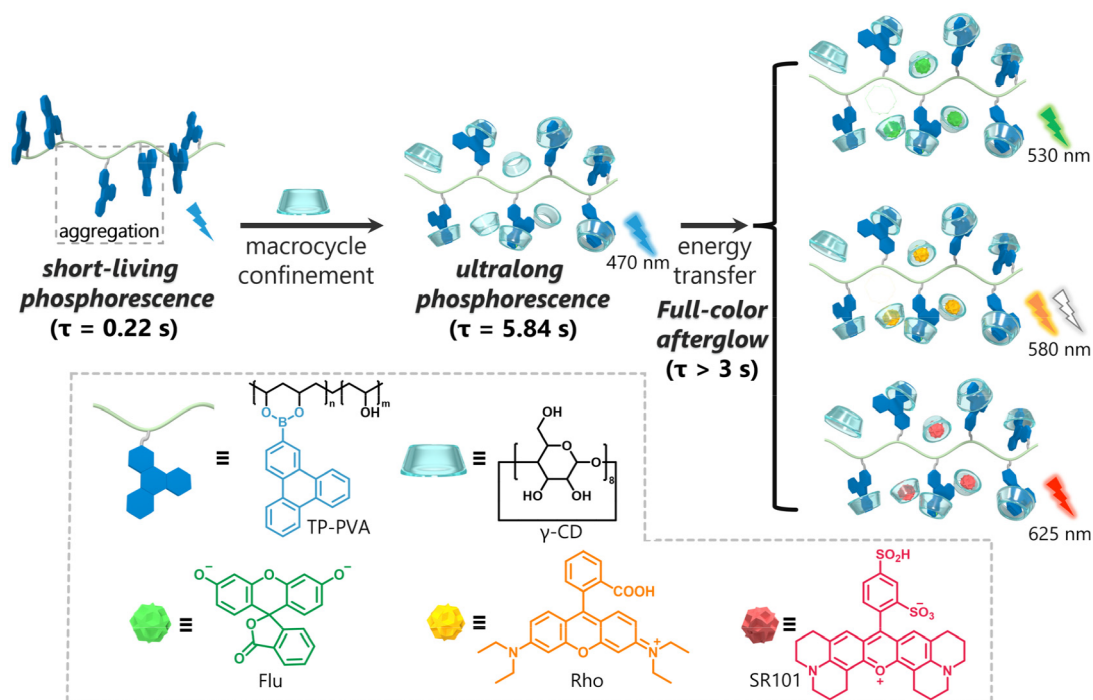
Scheme 1. Schematic Illustration of the Synergistic Assembly of TP-PVA/ γ -CD and the Formation of Full-Color Afterglow

Figure 1. (a) PL spectra and phosphorescence spectra of TP-PVA/ γ -CD films under ambient conditions (the mass ratio of TP and PVA is 1:100, the molar ratio of TP and γ -CD is 1:4; $\lambda_{\text{ex}} = 310 \text{ nm}$, delayed time = 1.5 ms); (b) time-resolved decay spectra of TP-PVA/ γ -CD with different PVA contents under ambient conditions (the molar ratio of TP and γ -CD is 1:4; $\lambda_{\text{ex}} = 310 \text{ nm}$, $\lambda_{\text{em}} = 468 \text{ nm}$); (c) phosphorescence lifetime with different PVA contents of TP-PVA films (red bars) and TP-PVA/ γ -CD films (blue bars) under ambient condition; (d) luminescence photographs of TP-PVA/ γ -CD film under ambient condition (the ambient condition is before and after ceasing 300 nm UV light).

(quenching concentration of the TP content in PVA film increased from 2 to 34 wt %). Benefiting from the high doping concentration of phosphorescence donors, efficient phosphorescence Förster resonance energy transfer (PRET) is achieved with a high donor/acceptor ratio ($[D]:[A] \geq 100:1$). In particular, by tuning the contents of energy acceptors fluorescein sodium (Flu), rhodamine B (Rho), or sulfonated rhodamine 101 (SR101), full-color afterglow emissions including blue, green, white, and red luminescence were achieved along with more than 50 s duration; these properties are among the best

results of organic afterglow systems, displaying uncommon pure organic afterglow behavior. Owing to mechanical flexibility and processability, the resulting polymeric materials can fabricate into security inks and various shapes of films with multifunctional applications. This hydrogen-bond-induced macrocycle-confined solid supramolecular strategy provides a new perspective to produce advanced multicolor afterglow materials.

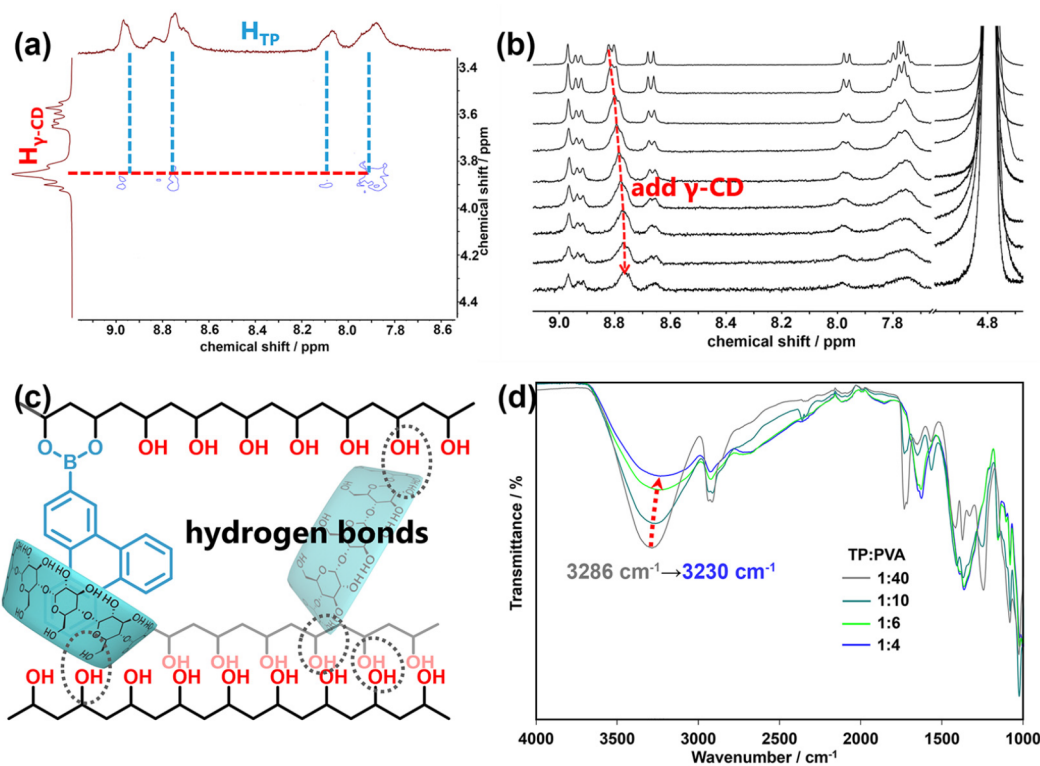


Figure 2. (a) Part of 2D ROESY (400 MHz, 298 K, D₂O with 15% DMSO-*d*₆) spectra of TP/γ-CD ([TP] = 1.0 mM, [γ-CD] = 10.0 mM). (b) ¹H NMR spectra of TP with different concentrations of γ-CD (400 MHz, 298 K, D₂O with 15% DMSO-*d*₆, [TP] + [γ-CD] = 5.0 mM and the ratio of [TP]:[γ-CD] from top to bottom is 9:1, 8:2, 7:3, 6:4, 5:5, 4:6, 3:7, 2:8, 1:9). (c) Schematic diagram of the hydrogen bond network enhanced by γ-CD. (d) Fourier transform infrared spectra of TP-PVA/γ-CD with different PVA contents.

RESULTS AND DISCUSSION

The TP-PVA/γ-CD aqueous solution was first prepared upon ultrasonic processing, and the resulting films were fabricated by casting these mixtures into quartz flakes and drying thoroughly. TP-PVA films without γ-CD exhibited two emission peaks around 368 nm (blue-purple band) and 465 nm (blue band) (Figure S1). Nanosecond-scale lifetimes indicated that the blue-purple band belonged to fluorescence (Figure S2). The gated emission spectra and seconds-scale lifetime at 465 nm indicated that the blue band belonged to phosphorescence (Figures S1 and S3). Similar to most phosphor-doped systems, ultralong phosphorescence properties were preserved at deficient doping concentrations, while the phosphorescence lifetime was significantly reduced when the mass ratio of TP was marginally increased (Figures S3 and 1c). Dramatically, the phosphorescence lifetime was weakened by about 24 times ($\tau_{\text{phos}} = 0.22$ s) when TP was 20.0 wt % (Figure 1c). In addition, the fluorescence peak occurred blunted and red-shifted as the PVA matrix mass ratio was reduced (Figure S4), implying that aggregates were formed at high phosphor concentrations. Cyclodextrin macrocycles have a strong bonding ability with polycyclic aromatic hydrocarbons, and isolation from γ-CD can prevent aggregation. To determine the molar ratio of TP and γ-CD, where cyclodextrin could effectively protect phosphorescence, the TP/γ-CD powders with different molar ratios were prepared. In Figure S5, the ultralong lifetime showed significant quenching with molar ratios below 1:4; thus, the molar ratio of TP and γ-CD (1:4) was used as a phosphorescence assembly in subsequent experiments. In the presence of γ-CD, the maximum lifetime of TP-PVA/γ-CD was prolonged from 5.24 to 5.84 s; meanwhile, the long-lived lifetime was maintained at over 5.3 s

even at high concentrations (Table S1). It is impressive that TP-PVA/γ-CD emitted an ultralong blue afterglow upon removing the exciting light, which could be captured by the naked eye and lasted 1 min (Figure 1d and Movie S1). Compared to the PL spectrum of TP-PVA, the fluorescence peaks of TP-PVA/γ-CD films stayed sharp and did not red-shift after reducing the PVA concentration, which indicated that γ-CD protected the TP from aggregation (Figure S6). Moreover, the phosphorescence spectrum of TP-PVA/γ-CD films was consistent with the RTP (room-temperature phosphorescence) spectrum of TP-PVA films, suggesting that the phosphorescence emission source of the TP-PVA/γ-CD film was from TP.

It is well-known that long-lived phosphorescence requires effective intersystem crossing (ISC) from S₁ to T_n and a slow nonradiative decay rate.^{38,39} Boronic acid derivatives have been widely researched as phosphorescent materials with excellent properties because the introduction of heteroatoms can enhance ISC efficiency via accelerating ¹(π, π*) → ³(n, π*) and ³(π, π*) → ¹(n, π*) transition.⁴⁰ Compared to the previous report,³³ TP-PVA/γ-CD displayed a much longer phosphorescence lifetime, implying that cyclodextrins as a matrix played a critical role in protecting the triplet excitons from quenching. To further confirm that high TP concentrations were prone to aggregation, we constructed absorption and fluorescence spectroscopy to investigate the effect of the solvent composition (H₂O/THF) on TP aggregation. In Figure S7, upon increasing the percentage of methanol in the unbound TP aqueous solution, the TP absorption peak was significantly enhanced and became sharp; meanwhile, the emission around 390 nm was blue-shifted and enhanced, which indicated that unbound triphenylene tended to aggregate in the aqueous solution. After the addition of γ-CD,

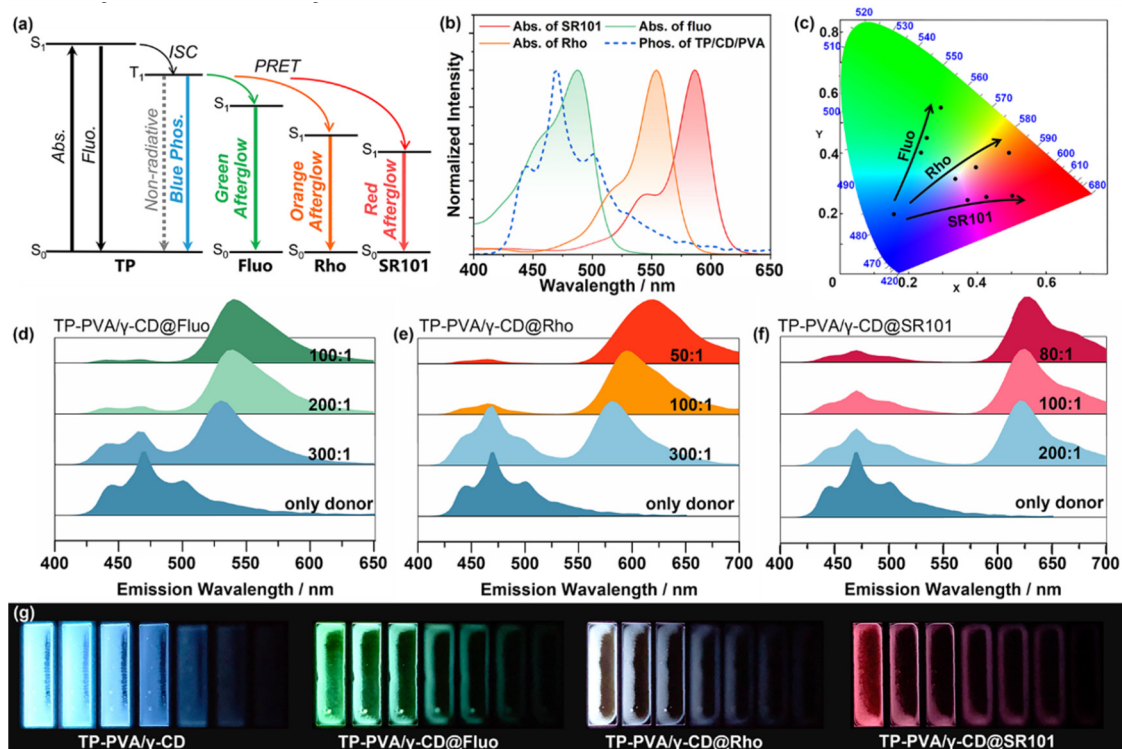


Figure 3. Luminous properties of TP-PVA/ γ -CD@acceptor-dyes films. (a) Simplified Jablonski diagram for ultralong phosphorescence and full-color energy transfer process. ISC, intersystem crossing. Abs., absorption. Fluo., fluorescence. Phos., phosphorescence. PRET, phosphorescence energy transfer. (b) Normalized phosphorescence spectrum ($\lambda_{\text{ex}} = 310$ nm, delayed time = 1.5 ms) of TP-PVA/ γ -CD (blue dashed line) and normalized absorption spectra of the energy acceptors in aqueous solution under ambient condition ([acceptor dyes] = 1.0×10^{-5} M, absorption spectra of Fluo indicated by the solid green line, absorption spectra of Rho indicated by the solid orange line, absorption spectra of SR101 indicated by the red solid line). (c) CIE 1931 chromaticity diagram of afterglow color changes when TP-PVA/ γ -CD was doped with different acceptor concentrations. (d–f) Delayed emission spectra of TP-PVA/ γ -CD with different acceptor concentrations under ambient conditions (left is TP-PVA/ γ -CD@Fluo, the middle is TP-PVA/ γ -CD@Rho, right is TP-PVA/ γ -CD@SR101, $\lambda_{\text{ex}} = 310$ nm, delayed time = 1.5 ms). (g) Full-color afterglow photographs of TP-PVA/ γ -CD@acceptor films doped with different acceptors under ambient conditions (first from the left is TP-PVA/ γ -CD films, $m_{\text{TP}}:m_{\text{PVA}} = 1:4$; second from the left is TP-PVA/ γ -CD@Fluo film, $m_{\text{TP}}:m_{\text{PVA}} = 1:4$, [TP]:[Fluo] is 100:1; third from the left is TP-PVA/ γ -CD@Rho films, $m_{\text{TP}}:m_{\text{PVA}} = 1:4$, [TP]:[Rho] is 300:1; fourth second from the left is TP-PVA/ γ -CD@SR101 film, $m_{\text{TP}}:m_{\text{PVA}} = 1:4$, [TP]:[SR101] is 100:1).

the absorption peak was enhanced significantly and became sharp; meanwhile, TP aqueous solutions changed from suspensions to clarified solutions (Figure S8). Transmission electron microscopy (TEM) provided more evidence for host–guest interaction to inhibit aggregation.

In Figure S9, TEM measurements showed that unbound TP aggregates into nanoparticles, while the TP/ γ -CD assemblies tend to disaggregate. The results of the TEM image as well as absorption and emission spectra indicated that adding γ -CD increased TP's solubility and inhibited its aggregation. Furthermore, assembly behaviors between TP and γ -CD were determined to demonstrate the role of γ -CD. UV–vis titration experiments were performed to determine the association constant (K_s), which is about 585 M^{-1} (Figure S10). It is noted that, in Figure S8, TP tends to aggregate due to poor solubility, which leads to absorption passivation because there is no base present in the solution. The bonding of CDs tends to deaggregate. In Figure S10, TP is completely soluble due to the presence of base, and the change in absorption is due to the bonding between monomeric TP and CD. Then, the ^1H NMR spectroscopy titration measurement was constructed; Job's plot was based on the resulting data (Figure S11), and the plot indicated that the host–guest binding stoichiometry was 1:1. ^1H NMR spectroscopy provided more details about bonding behaviors: as shown in Figure 2b, with the increase of the

concentration of γ -CD, the proton signals of TP shifted downfield from $\delta = 8.82$ ppm to $\delta = 8.76$ ppm, accompanied by shape changes, which indicated that TP was injected into the cavity of γ -CD (Figure 2b). The same conclusion was also confirmed by utilizing two-dimensional NMR analysis. Specifically, TP's ROESY (nuclear overhauser effect spectroscopy) spectra showed strong rotating frame nuclear Overhauser effect signals with $-\text{OH}$ of γ -CD (Figure 2a). To further confirm the role of host–guest interactions in enhancing phosphorescence, the adamantane derivative (Ada), one of the most strongly bound guests to cyclodextrin, was added to TP-PVA/ γ -CD to occupy the cyclodextrin cavity. The long-lived luminescence of TP-PVA/ γ -CD@Ada could be detected by the naked eye or by instruments (Figure S12); meanwhile, the fluorescence peak was red-shifted. These observations were similar to those without the addition of cyclodextrin, which implied that the host–guest interaction protected the long-lived phosphorescence from quenching at high doping concentrations.

To prove the existence of a covalent bond between the polymer and TP, we freeze-dried the polymer after the reaction and analyzed its ultraviolet absorption after thoroughly washing with organic solvent. The absorption peak of TP still existed, and it was calculated that about 61% of TP was covalently modified on the PVA based on absorption (Figure S13c). Without covalent modification, phosphorescence lifetimes occurred

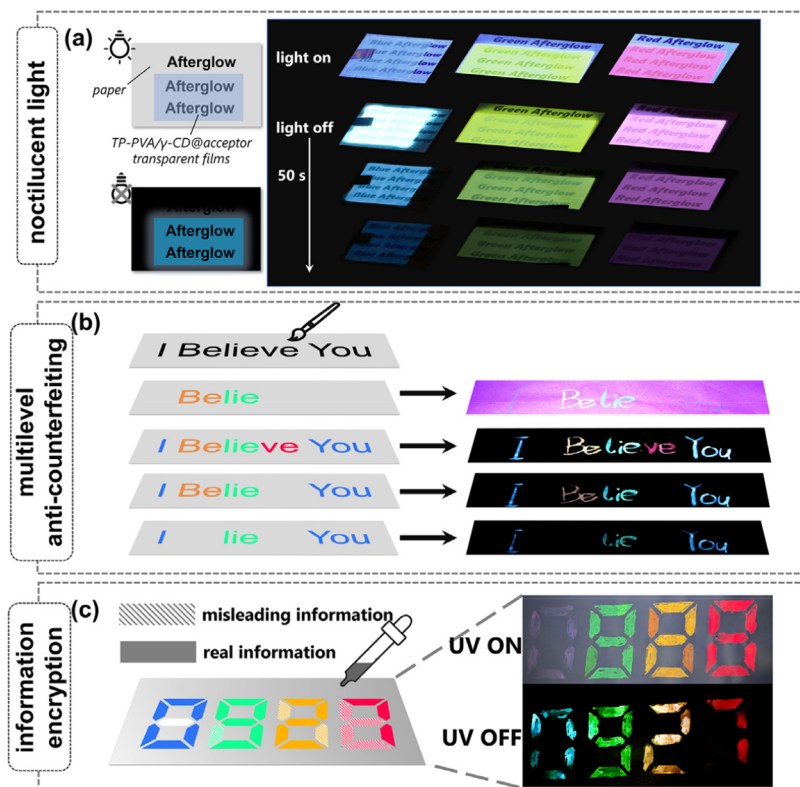


Figure 4. (a) Luminescence photographs of that TP-PVA/ γ -CD@acceptor transparent films were applied for a noctilucence light source ($m_{\text{TP}}:m_{\text{PVA}} = 1:20$, [TP]:[Fluo] is 100:1, [TP]:[Rho] is 100:1, [TP]:[SR101] is 100:1, the excitation light source is 300 nm hand-held lamp). (b) Schematic illustration of the application process for multilevel anticounterfeit application ($m_{\text{TP}}:m_{\text{PVA}} = 1:20$, [TP]:[Fluo] is 40:1, [TP]:[Rho] is 40:1, [TP]:[SR101] is 40:1, the excitation light source is a 300 nm hand-held lamp, print stock is paper with strong background fluorescence). (c) Schematic illustration of the application process for information encryption ($m_{\text{TP}}:m_{\text{PVA}} = 1:20$, [TP]:[Fluo] is 20:1, [TP]:[Rho] is 20:1, [TP]:[SR101] is 20:1, the excitation light source is a 300 nm hand-held lamp).

earlier and faster quenching occurred with increasing TP concentration, which implied that the covalent bonds between luminophores and polymers were an essential part of the rigid environment (Figure S13). The absence of covalent modification implied that the covalent bonds between luminophores and polymers were an essential part of the rigid environment (Figure S13). Besides covalent modification, the hydrogen bonding network provided by γ -CD and PVA suppressed the energy loss from molecular motion. First, we performed X-ray powder diffraction analysis to reveal the structures of TP-PVA/ γ -CD (1.0–50.0 wt %) since the microstructure (such as crystalline) of materials has a dramatic effect on their photophysical properties, and the results revealed that all of them were amorphous (Figure S14); furthermore, as the polymeric matrix mass fraction decreased, a distinct characteristic peak appeared, which indicates that the presence of γ -CD contributed to form a rigid and ordered environment. Then, Fourier transform infrared spectra provided additional evidence. In Figure 2d, the films containing different mass ratios of PVA exhibited a distinct peak at approximately 3286 cm^{-1} , attributed to the hydroxyl group between PVA and γ -CD. Notably, upon decreasing the polymer matrix mass ratio, the peak intensity at 3230 cm^{-1} shifted to shorter wavelengths and became notably wider. It is considered that the hydroxyl groups from cyclodextrins increased the degree of association of hydrogen bonding at high doping concentrations. To sum up, the B–O covalent bonding, the hydrogen bonding network formed between cyclodextrin and PVA, and the rigid cavity of

cyclodextrin provided an ideal environment for activating phosphorescence.

Generally, an efficient FRET process requires positioning in proximity of each other, and an excellent match to the spectra of the donor emission and the receptor absorption.⁴¹ The features, including a high doping ratio and broad blue phosphorescence emission ranging from 400 to 600 nm, motivate us to construct phosphorescence energy transfer systems. To achieve afterglow color transfer, green dye Flu, orange dye Rho and red dye SR101 were chosen as triplet energy acceptors because their absorption spectra have a good overlap with the phosphorescence spectrum of TP-PVA/ γ -CD (Figure 3b), which satisfies the premise for energy transfer. TP-PVA/ γ -CD_{1:4} (the mass ratio of TP and PVA is 1:4) was selected as a long-lived phosphorescence donor material. As the ratios of energy receptor dyes increased, TP-PVA/ γ -CD@Flu, TP-PVA/ γ -CD@Rho, and TP-PVA/ γ -CD@SR101 exhibited emitting color transformations ranging from blue to green, orange, or red (Figure 3c); meanwhile, the intensity of the donors' phosphorescence peak became weaker, and the intensity of the acceptors' delayed fluorescence peak of the receptor became more robust in the phosphorescence spectrum, which implied the high-efficiency energy transfer from the donor to the acceptor (Figures 3d–f). Impressively, when the molar ratio of the donor and acceptor was 200:1, TP-PVA/ γ -CD@Flu exhibited green afterglow ($\tau = 3.99\text{ s}$) upon removing the exciting light; when the molar ratio of donor and acceptor was 300:1, TP-PVA/ γ -CD@Rho exhibited persistent white luminescence ($\tau = 3.34\text{ s}$) upon removing the exciting light, and when the ratio is 100:1, the color of afterglow further converted

to orange ($\tau = 3.02$ s). When the donor and acceptor molar ratio is 100:1, TP-PVA/ γ -CD@SR101 is exhibited upon removal of the exciting light. In addition, compared to the high donor concentration doping system (TP-PVA/ γ -CD_{1:4}, in which the mass ratio of TP and PVA is 1:4), a higher concentration of acceptor was required to achieve the afterglow color transformation at a low donor concentration doping system (TP-PVA/ γ -CD_{1:100} in which the mass ratio of TP and PVA is 1:100). In Figure S18, the receptor concentrations had to be increased at least 10, 20, or 80 times to achieve the afterglow color change from blue to green, orange, or red; meanwhile, the lifetime of the afterglow was significantly reduced (Figure S19). Significant afterglow quenching might result from the higher acceptor concentration required to diminish the distance between D–A at a low donor concentration doping system, and high acceptor concentrations lead to quenching of long-lived triplet excitons. The steady-state and delayed spectra upon doping with acceptor dyes were investigated to demonstrate that the energy transfer came from the triplet state to the single state. In Figure S20, emission peaks for dyes, Fluo, Rho, and SR101, were kept the same at steady-state and delayed spectra. On the other hand, there was no significant change in the fluorescence lifetime of both the donor and the acceptor after changing the D–A doping ratio (Tables S2–S4). And these results indicated that both the TP and the acceptor dye absorbed the energy of the excitation light (Figure S21), and then the radiative transition of TP was in the form of fluorescence and phosphorescence; however, the radiation transition of the acceptor dye was only in the form of fluorescence. In addition, one of the most important forms is triplet-to-singlet FRET, in which the long-lived TP triplet energy directly transfers to the singlet state of the acceptor to result in persistent delayed fluorescence.

Macrocycles played an indispensable role in promoting the fluorescence lifetime; concretely, apart from that, the hydroxyl groups from cyclodextrins promoted the association of hydrogen bonding, and the host–guest interaction between γ -CD and acceptor dyes might protect the PRET process. In Figure S23 and S24, upon adding γ -CD, the chemical shifts of the acceptor's protons were shifted to varying degrees. Furthermore, the fluorescence intensities of the acceptor were enhanced. The results of fluorescence titration and ¹H NMR spectroscopy indicated that γ -CD could effectively bind to acceptor dyes and enhance luminescence. In sum, γ -CD not only enhances the rigid environment through hydrogen bonding but also confines the D–A chromophore through universal host–guest interaction, thus promoting ultralong tunable afterglow.

These polymeric materials could be processed into multi-color-emitting flexible films by taking advantage of the excellent film-formation and water-solubility. Remarkably, the flexible nature of the afterglow films allows repeated bending and flexing; meanwhile, films retain stable long-lived afterglow emission (Movie S2). Furthermore, the full-color afterglow objects can be easily prepared by rolling and folding (Figure S25 and Movie S3). The transparent films could be used as a noctilucous light source under ambient conditions; as shown in Figure 4a, the films doped with different acceptor dyes were covered on the paper. After removal of the light source, the naked eye could still capture the “afterglow” words within 50 s (Movie S4).

In addition, given the multicolor emission and time-dependent luminescence, hand-writable ink was successfully prepared and applied for multilevel anticounterfeiting and information encryption, respectively. As shown in Figure 4b, a

sentence of “I believe you” was written on paper, and only “Belie” can be identified under a UV lamp because of the substantial interference of background fluorescence from the printing paper; then the first level of information “I Believe You” is revealed when the UV light is removed; after a short period, the information that the naked eye can capture becomes “I Belie You”; and the fourth level of information will be displayed in about half a minute, and the sentence turned into “I lie You”. It is worth mentioning that, due to the hygroscopic nature of PVA, the afterglow property will disappear after about 10 min of exposure to air. Finally, the individual acceptor fluorescent dyes and TP-PVA/ γ -CD@acceptor solutions were prepared and brushed on paper. The acceptor dyes solutions were used for misleading information because of the short-living lifetime, and the TP-PVA/ γ -CD@acceptor solutions were used for brushing real information. As shown in Figure 4c, the integrated number “0888” was brushed on paper. The wrong information, “0888” was observed under the UV light while the real information, “0927” was revealed after removing the lighting source. Consequently, such a double information encryption was realized.

CONCLUSIONS

In summary, a series of persistent luminescence films based on macrocycle confinement were developed through doping different D–A dyes into a cyclodextrin-confined polymer matrix. These polymer-based films displayed a full-color afterglow duration of >50 s under ambient conditions. The principle of this strategy leans upon the rigid environment from the coassembly between the γ -CD and PVA chains, as well as the confined bonding between the chromophores and γ -CD, effectively suppressing the nonradiative decay and promoting the triplet state to the single state energy transfer process. The construction of supramolecular-confinement polymers will broaden multifunctional materials and expand phosphorescence materials applications.

METHODS

All reagents and solvents were purchased from commercial suppliers and used as supplied unless otherwise noted. ¹H NMR was performed with an Ascend 400 MHz instrument. NOESY spectra were measured on a ZhongKe-Oxford I-400 instrument. UV–vis absorption spectra were recorded on a Shimadzu UV-3600 spectrophotometer with a PTC-348WI temperature controller in a quartz cell (light path 10 mm) at 298 K. Photoluminescence (PL) spectra, time-correlated decay profiles, and quantum efficiency were processed on an Edinburgh Instruments FSS apparatus (Livingstone, UK). Fourier transform infrared spectra were processed on a Tensor II instrument (Bruker). TEM experiments were carried out on an FEI Tecnai G2 F20 microscope operating at 200 kV. XRD patterns were obtained at a Rigaku SmartLab 3K instrument. All measurements were carried out at room temperature (RT) unless specified otherwise. The Commission International de l'Eclairage (CIE) 1931 chromaticity diagram was obtained on FLS1000 software. All afterglow photos and videos were recorded with a mobile device.

ASSOCIATED CONTENT

Supporting Information

The Supporting Information is available free of charge at <https://pubs.acs.org/doi/10.1021/jacsau.3c00255>.

Detailed experiments included synthetic procedures, behavior characterization for assemblies, and characterization of luminous properties for assemblies and characterization data (PDF)

Movie showing ultralong blue afterglow of TP-PVA/g-CD upon removal of light (MOV)

Movie showing the flexible nature of afterglow films (MOV)

Movie showing different preparations of full-color afterglow objects (MOV)

Movie showing the presence of visible multicolor afterglow with 50 s duration (MOV)

AUTHOR INFORMATION

Corresponding Author

Yu Liu – College of Chemistry, State Key Laboratory of Elemento Organic Chemistry, Nankai University, Tianjin 300071, P. R. China; Haihe Laboratory of Sustainable Chemical Transformations, Tianjin 300071, P. R. China; Collaborative Innovation Center of Chemical Science and Engineering, Tianjin 300071, P. R. China; orcid.org/0000-0001-8723-1896; Email: yuliu@nankai.edu.cn

Authors

Xin-Kun Ma – College of Chemistry, State Key Laboratory of Elemento Organic Chemistry, Nankai University, Tianjin 300071, P. R. China

Qingwen Cheng – College of Chemistry, State Key Laboratory of Elemento Organic Chemistry, Nankai University, Tianjin 300071, P. R. China; Haihe Laboratory of Sustainable Chemical Transformations, Tianjin 300071, P. R. China; Collaborative Innovation Center of Chemical Science and Engineering, Tianjin 300071, P. R. China

Xiaolu Zhou – College of Chemistry, State Key Laboratory of Elemento Organic Chemistry, Nankai University, Tianjin 300071, P. R. China

Complete contact information is available at:
<https://pubs.acs.org/10.1021/jacsau.3c00255>

Author Contributions

X.-K.M. conceived and designed the experiments. X.-K.M. and Q.C. performed the characterization. X.-K.M. wrote the main manuscript. X.Z. provided help in revising the manuscript. Y.L. supervised the work and edited the manuscript. All authors analyzed and discussed the results and reviewed the manuscript.

Notes

The authors declare no competing financial interest.

ACKNOWLEDGMENTS

We thank National Nature Science Foundation of China (NNSFC, Grant Nos. 22131008) and China Fundamental Research Funds for the Central Universities.

REFERENCES

- (1) Xu, S.; Chen, R.; Zheng, C.; Huang, W. Excited State Modulation for Organic Afterglow: Materials and Applications. *Adv. Mater.* **2016**, *28*, 9920.
- (2) Wang, Z.; Gao, L.; Zheng, Y.; Zhu, Y.; Zhang, Y.; Zheng, X.; Wang, C.; Li, Y.; Zhao, Y.; Yang, C. Four-in-One Stimulus-Responsive Long-Lived Luminescent Systems Based on Pyrene-Doped Amorphous Polymers. *Angew. Chem., Int. Ed.* **2022**, e202203254.
- (3) Louis, M.; Thomas, H.; Gmelch, M.; Haft, A.; Fries, F.; Reineke, S. Blue-Light-Absorbing Thin Films Showing Ultralong Room-Temperature Phosphorescence. *Adv. Mater.* **2019**, *31*, 1807887.
- (4) Nidhankar, A. D.; Goudappagouda; Wakchaure, V. C.; Babu, S. S. Efficient metal-free organic room temperature phosphors. *Chem. Sci.* **2021**, *12*, 4216.
- (5) Hirata, S. Recent Advances in Materials with Room-Temperature Phosphorescence: Photophysics for Triplet Exciton Stabilization. *Adv. Opt. Mater.* **2017**, *5*, 1700116.
- (6) Kenry; Chen, C. J.; Liu, B. Enhancing the performance of pure organic room-temperature phosphorescent luminophores. *Nat. Commun.* **2019**, *10*, 2111.
- (7) Ma, X.; Wang, J.; Tian, H. Assembling-Induced Emission: An Efficient Approach for Amorphous Metal-Free Organic Emitting Materials with Room Temperature Phosphorescence. *Acc. Chem. Res.* **2019**, *52*, 738.
- (8) Kwon, M. S.; Yu, Y.; Coburn, C.; Phillips, A. W.; Chung, K.; Shanker, A.; Jung, J.; Kim, G.; Pipe, K.; Forrest, S. R.; Youk, J. H.; Gierschner, J.; Kim, J. Suppressing molecular motions for enhanced room-temperature phosphorescence of metal-free organic materials. *Nat. Commun.* **2015**, *6*, 8947.
- (9) Gu, L.; Wu, H. W.; Ma, H. L.; Ye, W. P.; Jia, W. Y.; Wang, H.; Chen, H. Z.; Zhang, N.; Wang, D. D.; Qian, C.; An, Z. F.; Huang, W.; Zhao, Y. L. Color-tunable ultralong organic room temperature phosphorescence from a multicomponent copolymer. *Nat. Commun.* **2020**, *11* (8), 944.
- (10) Zhu, Y.; Guan, Y.; Niu, Y. F.; Wang, P.; Chen, R. J.; Wang, Y. H.; Wang, P.; Xie, H. L. Ultralong Polymeric Room Temperature Phosphorescence Materials Fabricated by Multiple Hydrogen Bondings Resistant to Temperature and Humidity. *Adv. Opt. Mater.* **2021**, *9*, 2100782.
- (11) Ma, X.; Xu, C.; Wang, J.; Tian, H. Amorphous Pure Organic Polymers for Heavy-Atom-Free Efficient Room-Temperature Phosphorescence Emission. *Angew. Chem., Int. Ed.* **2018**, *57*, 10854.
- (12) Cai, S.; Sun, Z.; Wang, H.; Yao, X.; Ma, H.; Jia, W.; Wang, S.; Li, Z.; Shi, H.; An, Z.; Ishida, Y.; Aida, T.; Huang, W. Ultralong Organic Phosphorescent Foams with High Mechanical Strength. *J. Am. Chem. Soc.* **2021**, *143*, 16256.
- (13) Guo, J.; Yang, C.; Zhao, Y. Long-Lived Organic Room-Temperature Phosphorescence from Amorphous Polymer Systems. *Acc. Chem. Res.* **2022**, *55*, 1160–1170.
- (14) Zhang, Y.; Chen, X.; Xu, J.; Zhang, Q.; Gao, L.; Wang, Z.; Qu, L.; Wang, K.; Li, Y.; Cai, Z.; Zhao, Y.; Yang, C. Cross-Linked Polyphosphazene Nanospheres Boosting Long-Lived Organic Room-Temperature Phosphorescence. *J. Am. Chem. Soc.* **2022**, *144*, 6107–6117.
- (15) Bolton, O.; Lee, K.; Kim, H.-J.; Lin, K. Y.; Kim, J. Activating efficient phosphorescence from purely organic materials by crystal design. *Nature. Chem.* **2011**, *3*, 205.
- (16) Gu, L.; Shi, H.; Bian, L.; Gu, M.; Ling, K.; Wang, X.; Ma, H.; Cai, S.; Ning, W.; Fu, L.; Wang, H.; Wang, S.; Gao, Y.; Yao, W.; Huo, F.; Tao, Y.; An, Z.; Liu, X.; Huang, W. Colour-tunable ultra-long organic phosphorescence of a single-component molecular crystal. *Nat. Photonics.* **2019**, *13*, 406.
- (17) Zhou, X. L.; Xu, S. L.; Liu, L. Q.; Sun, Y. P.; Cheng, J. X.; Duan, X. Y.; Zhou, L. S.; Qu, H. M. 5,5-Dioxo-phenothiazine-based D-A-D type AIE molecules enabling persistent room temperature phosphorescence, white light emission and dual-mode mechanochromism. *Dyes Pigm.* **2021**, *188*, 109193.
- (18) Ma, X.-K.; Liu, Y. Supramolecular Purely Organic Room-Temperature Phosphorescence. *Acc. Chem. Res.* **2021**, *54*, 3403.
- (19) Huo, M.; Dai, X.-Y.; Liu, Y. Ultrahigh Supramolecular Cascaded Room-Temperature Phosphorescence Capturing System. *Angew. Chem., Int. Ed.* **2021**, *60*, 27171–27177.
- (20) Ma, X. K.; Zhou, X. L.; Wu, J.; Shen, F. F.; Liu, Y. Two-Photon Excited Near-Infrared Phosphorescence Based on Secondary Supramolecular Confinement. *Adv. Sci.* **2022**, *9*, 2201182.
- (21) Liu, S.; Lin, Y.; Yan, D. Hydrogen-Bond Organized 2d Metal-Organic Microsheets: Direct Ultralong Phosphorescence and Color-Tunable Optical Waveguides. *Sci. Bull.* **2022**, *67*, 2076–2084.
- (22) Nie, F.; Wang, K.-Z.; Yan, D. Supramolecular Glasses with Color-Tunable Circularly Polarized Afterglow through Evaporation-Induced

Self-Assembly of Chiral Metal-Organic Complexes. *Nat. Commun.* **2023**, *14*, 1654.

(23) Nie, F.; Yan, D. Macroscopic Assembly of Chiral Hydrogen-Bonded Metal-Free Supramolecular Glasses for Enhanced Color-Tunable Ultralong Room Temperature Phosphorescence. *Angew. Chem., Int. Ed.* **2023**, *62*, No. e202302751.

(24) Zhang, Z.-Y.; Chen, Y.; Liu, Y. Efficient Room-Temperature Phosphorescence of a Solid-State Supramolecule Enhanced by Cucurbit[6]uril. *Angew. Chem., Int. Ed.* **2019**, *58*, 6028–6032.

(25) Ma, X.-K.; Zhang, Y.-M.; Yu, Q.; Zhang, H.; Zhang, Z.; Liu, Y. A twin-axial pseudorotaxane for phosphorescence cell imaging. *Chem. Commun.* **2021**, *57*, 1214.

(26) Li, D.; Lu, F.; Wang, J.; Hu, W.; Cao, X.-M.; Ma, X.; Tian, H. Amorphous metal-free room-temperature phosphorescent small molecules with multicolor photoluminescence via a host-guest and dual-emission strategy. *J. Am. Chem. Soc.* **2018**, *140*, 1916–1923.

(27) Connors, K. A. The Stability of Cyclodextrin Complexes in Solution. *Chem. Rev.* **1997**, *97*, 1325–1358.

(28) Scypinski, S.; Love, L. J. C. Cyclodextrin-induced room-temperature phosphorescence of nitrogen heterocycles and bridged biphenyls. *Anal. Chem.* **1984**, *56*, 331–336.

(29) Turro, N. J.; Bolt, J. D.; Kuroda, Y.; Tabushi, I. A Study of The Kinetics of Inclusion of Halonaphthalenes with β -cyclodextrin via Time Correlated Phosphorescence. *Photochem. Photobiol.* **1982**, *35*, 69–72.

(30) Dang, Q.; Jiang, Y.; Wang, J.; Wang, J.; Zhang, Q.; Zhang, M.; Luo, S.; Xie, Y.; Pu, K.; Li, Q.; Li, Z. Room-Temperature Phosphorescence Resonance Energy Transfer for Construction of Near-Infrared Afterglow Imaging Agents. *Adv. Mater.* **2020**, *32*, 2006752.

(31) Hayashi, K.; Fukasawa, K.; Yamashita, T.; Hirata, S. Rational Design of a Triplet Afterglow Sensitizer Allowing for Bright Long-Wavelength Afterglow Room-Temperature Emission. *Chem. Mater.* **2022**, *34*, 1627.

(32) Kuila, S.; George, S. J. Phosphorescence Energy Transfer: Ambient Afterglow Fluorescence from Water-Processable and Purely Organic Dyes via Delayed Sensitization. *Angew. Chem., Int. Ed.* **2020**, *59*, 9393.

(33) Lin, F.; Wang, H.; Cao, Y.; Yu, R.; Liang, G.; Huang, H.; Mu, Y.; Yang, Z.; Chi, Z. Stepwise Energy Transfer: Near-Infrared Persistent Luminescence from Doped Polymeric Systems. *Adv. Mater.* **2022**, *34*, 2108333.

(34) Peng, H.; Xie, G.; Cao, Y.; Zhang, L.; Yan, X.; Zhang, X.; Miao, S.; Tao, Y.; Li, H.; Zheng, C.; Huang, W.; Chen, R. On-demand modulating afterglow color of water-soluble polymers through phosphorescence FRET for multicolor security printing. *Sci. Adv.* **2022**, *8*, No. eabk2925.

(35) Kirch, A.; Gmelch, M.; Reineke, S. Simultaneous Singlet-Singlet and Triplet-Singlet Förster Resonance Energy Transfer from a Single Donor Material. *J. Phys. Chem. Lett.* **2019**, *10*, 310–315.

(36) Ma, L.; Xu, Q.; Sun, S.; Ding, B.; Huang, Z.; Ma, X.; Tian, H. A Universal Strategy for Tunable Persistent Luminescent Materials Via Radiative Energy Transfer. *Angew. Chem., Int. Ed.* **2022**, *61*, No. e20211574.

(37) Zhao, Y.; Ma, L.; Huang, Z.; Zhang, J.; Willner, I.; Ma, X.; Tian, H. Visible Light Activated Organic Room-Temperature Phosphorescence Based on Triplet-to-Singlet Förster-Resonance Energy Transfer. *Adv. Opt. Mater.* **2022**, *10*, 2102701.

(38) Ma, H.; Peng, Q.; An, Z.; Huang, W.; Shuai, Z. Efficient and Long-Lived Room-Temperature Organic Phosphorescence: Theoretical Descriptors for Molecular Designs. *J. Am. Chem. Soc.* **2019**, *141*, 1010–1015.

(39) Zhao, W.; He, Z.; Tang, B. Z. Room-temperature phosphorescence from organic aggregates. *Nat. Rev. Mater.* **2020**, *5*, 869.

(40) Hackney, H. E.; Perepichka, D. F. Recent advances in room temperature phosphorescence of crystalline boron containing organic compounds. *Aggregate* **2022**, e123.

(41) Wu, L.; Huang, C.; Emery, B. P.; Sedgwick, A. C.; Bull, S. D.; He, X.-P.; Tian, H.; Yoon, J.; Sessler, J. L.; James, T. D. Förster resonance

energy transfer (FRET)-based small-molecule sensors and imaging agents. *Chem. Soc. Rev.* **2020**, *49*, 5110–5139.